

Identification and Functional Characterization of Allosteric Agonists for the G Protein-Coupled Receptor FFA2

Taeweon Lee, Ralf Schwandner, Gayathri Swaminath, Jennifer Weiszmann, Mario Cardozo, Joanne Greenberg, Peter Jaeckel, Hongfei Ge, Yingcai Wang, Xianyun Jiao, Jiwen Liu, Frank Kayser, Hui Tian, and Yang Li

Amgen Inc., South San Francisco, California (T.L., G.S., J.W., M.C., J.G., H.G., Y.W., X.J., J.L., F.K., H.T., Y.L.); and Amgen Research GmbH, Regensburg, Germany (R.S., P.J.)

Received June 6, 2008; accepted September 25, 2008

ABSTRACT

FFA2 (GPR43) has been identified as a receptor for short-chain fatty acids (SCFAs) that include acetate and propionate. FFA2 is highly expressed in islets, a subset of immune cells, and adipocytes. Although the potential roles of FFA2 activation in these tissues have previously been described, the physiological functions are still unclear. The potency for SCFAs on FFA2 is low, in the high micromolar to millimolar concentrations. To identify better pharmacological tools to study receptor function, we used high-throughput screening (HTS) to discover a series of small molecule phenylacetamides as novel and more potent FFA2 agonists. This series is specific for FFA2 over FFA1 (GPR40) and FFA3 (GPR41), and it is able to activate both the G_{α_q} and G_{α_i} pathways in vitro on Chinese hamster ovary cells stably expressing FFA2. Treatment of adipocytes with these compounds also resulted in G_{α_i} -dependent inhibition of lipoly-

sis similar to that of endogenous ligands (SCFAs). It is noteworthy that these compounds not only acted as FFA2 agonists but also exhibited positive cooperativity with acetate or propionate. The observed allosteric modulation was consistent in all the functional assays that we have explored, including cAMP, calcium mobilization, guanosine 5'-[γ -thio]triphosphate binding, and lipolysis. Molecular modeling analysis of FFA2 based on human β_2 -adrenergic receptor structure revealed potential nonoverlapping binding sites for the endogenous and synthetic ligands, further providing insight into the binding pocket for the allosteric interactions. This is the first report describing the identification of novel allosteric modulators with agonist activity for FFA2, and these compounds may serve as tools for further unraveling the physiological functions of the receptor and its involvement in various diseases.

The superfamily of G protein-coupled receptors (GPCRs) is one of the largest families of proteins in the mammalian genome and shares a conserved structure composed of seven transmembrane helices (Fredriksson et al., 2003, Fredriksson and Schioth, 2005). The discovery of drugs acting on GPCRs has been extremely successful, with 50% of all recently launched drugs having activities against GPCR targets and annual world wide sales exceeding \$50 billion (Lundstrom, 2006). Thus, this family of proteins is attractive for biopharmaceutical research. FFA2 (GPR43) is a member of a subfamily of related GPCRs clustered at chromosome 19q13.1 in humans (Sawzdargo et al., 1997). The subfamily members—FFA1 (GPR40), FFA3 (GPR41), and FFA2 (GPR43)—have recently been identified as re-

ceptors for fatty acids (Covington et al., 2006). The three members of this subfamily share ~30 to 40% sequence identity with specificity toward different fatty acid carbon chain lengths, with short-chain fatty acids (SCFAs, six or shorter carbon molecules) activating FFA2 and FFA3, and medium- and long-chain fatty acids activating FFA1 (Rayasam et al., 2007). Although both FFA2 and FFA3 are activated by SCFAs, FFA2 and FFA3 show differences in SCFA specificity, intracellular signaling, and tissue localization. FFA2 can couple to both G_{α_i} and G_{α_q} , whereas FFA3 couples only to G_{α_i} (Brown et al., 2003, Le Poul et al., 2003, Nilsson et al., 2003). In addition, C2 (acetate) and C3 (propionate) are the most potent activators of FFA2, whereas C2 is not as potent as C3, C4, or C5 against FFA3 (Brown et al., 2003, Le Poul et al., 2003).

FFA2 expression has been reported to be enriched in immune cells and adipocytes (Brown et al., 2003, Le Poul et al., 2003, Nilsson et al., 2003, Hong et al., 2005, Ge et al., 2008).

T.L., R.S., G.S., and J.W. contributed equally to this work.

Article, publication date, and citation information can be found at <http://molpharm.aspetjournals.org>.
doi:10.1124/mol.108.049536.

ABBREVIATIONS: GPCR, G protein-coupled receptor; SCFA, short-chain fatty acid; HTS, high-throughput screen; GTP- γ S, guanosine 5'-[γ -thio]triphosphate; DMSO, dimethyl sulfoxide; CHO, Chinese hamster ovary; TM, transmembrane domain; PTX, pertussis toxin; CGP7930, 2,6-di-*tert*-butyl-4-(3-hydroxy-2,2-dimethylpropyl)phenol; RLU, relative luminescence units.

Given the well established effects of SCFAs on leukocytes, it has been suggested that FFA2 may play a role in various immune and inflammatory responses (Brown et al., 2003, Le Poul et al., 2003, Nilsson et al., 2003). FFA2 is also induced during adipocyte differentiation and exhibits increased levels during high-fat feeding in rodents, suggesting that FFA2 may affect adipocyte function as well (Hong et al., 2005). Indeed, it has recently been reported that acetate and propionate may stimulate adipogenesis and inhibit lipolysis in adipocytes via FFA2 activation (Hong et al., 2005, Ge et al., 2008). In addition, we have previously shown that activation of FFA2 results in the reduction of plasma FFA levels in vivo (Ge et al., 2008). Given the similarity in activity on adipocytes to the nicotinic acid receptor, GPR109A, and the beneficial effects of nicotinic acid treatment on raising high-density lipoprotein levels, improvements in multiple cardiovascular risk factors, and overall reduction in mortality (Carlson, 2005), FFA2 could also potentially function to modulate aspects of metabolic disorders. However, because of the low potency of the endogenous ligands, it has previously been challenging to further explore the functions of FFA2 in various diseases.

To better understand the pharmacological functions of FFA2, we conducted a high-throughput screen (HTS) and identified a series of phenylacetamide derivatives as FFA2 agonists. Here, we describe the identification and characterization of this novel series of FFA2 ligands and their potential utility in further understanding the receptor function.

Materials and Methods

Materials. [35 S]guanosine 5'-[γ -thio]triphosphate (GTP γ S; 1250 Ci/mmol) was purchased from PerkinElmer Life and Analytical Sciences (Waltham, MA). Unlabeled GTP γ S was obtained from Roche Molecular Biochemicals (Indianapolis, IN). GDP, forskolin, and sodium acetate were purchased from Sigma (St. Louis, MO). Propionate was obtained from Fluka Chemie (Taufkirchen, Germany), and pertussis toxin was from EMD Biosciences (San Diego, CA). Coelenterazine was from P.J.K. GmbH (Kleinblittersdorf, Germany). HitHunter cAMP XS assay kit was purchased from GE Healthcare (Chalfont St. Giles, Buckinghamshire, UK). Phenylacetamides 1 and 2 were synthesized at Amgen, Inc. The detailed synthetic routes will be described elsewhere (Y. Wang, personal communication). Phenylacetamides 1 and 2 were completely soluble in dimethyl sulfoxide (DMSO) and were stable at 10 mM. The 10 mM stock solution was then subsequently diluted into media or buffer to final concentrations as indicated in the figures. The final DMSO concentrations in the media of all cell-based assays were 0.1% (v/v) and in GTP γ S binding assay was 1% (v/v). Same final DMSO concentrations were also maintained in no compound control cells or reactions to eliminate any potential solvent effects. No precipitation of compounds were observed either in media or in reaction buffers under the conditions described here.

Cell Line Development and Aequorin Assay. The bicistronic expression plasmid pIRES (Clontech, Mountain View, CA) containing the coding sequence of the human FFA2 receptor was transfected using Fugene6 (Roche Diagnostics GmbH, Mannheim, Germany) in CHO-K1 cells stably expressing the mitochondrial targeted aequorin. Resistant clones were obtained by single colony separation and compared for their response to a reference agonist using the aequorin assay. The cell-based receptor-dependent aequorin assay was used in a high throughput screen of a compound library as described previously (An et al., 1998) with slight modification. In this assay, agonist-induced receptor activation was determined by an increase in cytosolic calcium concentration released from intracellu-

lar calcium stores. The increased cytosolic calcium was monitored by luminescence emitted from aequorin.

Lipolysis Assay in Differentiated 3T3 L1 Cells. 3T3L1 cells (American Type Culture Collection, Manassas, VA) were cultured in DMEM with 10% (v/v) FCS on Corning CellBind 96-well plates. Upon confluence, differentiation was induced by adding 250 nM dexamethasone, 500 μ M isobutylmethylxanthine, 1 μ g/ml insulin, 2 nM triiodothyronine, and 0.3 μ M rosiglitazone into basic culture medium for 2 days. The cells were then cultured in DMEM with 10% (v/v) FCS with 1 μ g/ml insulin, 2 nM T3, and 0.3 μ M rosiglitazone for two days and maintained in basic culture medium thereafter. Fifteen days after induction, differentiated adipocytes were preincubated with Krebs-Ringer bicarbonate and 25 mM HEPES (KRH buffer; Sigma) with 0.01% (w/v) fatty-acid free BSA (Sigma) and 1 unit/ml adenosine deaminase (Codexis, Pasadena, CA) for 2 h. Cells were then treated with compounds in KRH buffer for 4 h. Glycerol released from lipolysis during treatment was measured by free glycerol reagent (Sigma).

cAMP Inhibition Assay. Inhibition of cAMP response was measured in CHO cells stably expressing human FFA2 via HitHunter cAMP XS assay kit (GE Healthcare). In brief, cells resuspended (10,000 in 10 μ l/well) in Hank's balanced salt solution (137 mM NaCl, 5.4 mM KCl, 0.25 mM Na₂HPO₄, 0.44 mM KH₂PO₄, 1.3 mM CaCl₂, and 1.0 mM MgSO₄) with 25 mM HEPES and 0.01% (w/v) BSA were stimulated with forskolin (5 μ M final in 5 μ l/well) in the presence of serially diluted test ligands (5 μ l/well) in a 384-well Optiplate (Perkin Elmer) at room temperature for 30 min before adding antibody and lysis reagents according to manufacturer's protocol. For allosteric activity studies, test ligands were 3-fold serially diluted and added to the above agonist concentration response reactions. The plates were further incubated in the dark overnight after adding detection solution, and read in CLIPR (Molecular Devices) for 1 min per plate. Data were expressed as Relative Luminescence Unit (RLU).

Membrane Preparation. Membranes were prepared from CHO cells stably expressing FFA2. CHO-FFA2 stable cells were pretreated with or without pertussis toxin (100 ng/ml) for 16 h before harvesting. All the membrane preparation steps were done at 4°C. In brief, cells were harvested by centrifugation (10 min at 10,000g), washed once with phosphate-buffered saline, and recentrifuged. Cells were later resuspended in lysis buffer (10 mM Tris-HCl, pH 7.4, with 1 mM EDTA) and lysed using 25 strokes of a Dounce homogenizer. Nuclei and unbroken cells were removed by centrifugation (5 min at 500g). The supernatant was removed and centrifuged (30 min at 40,000g). The resulting pellet was resuspended in 20 ml of lysis buffer (10 mM Tris-HCl, pH 7.4, alone) and recentrifuged. Membranes were resuspended at 0.5 to 1.5 mg of protein/ml in binding buffer (20 mM HEPES pH 7.5, 5 mM MgCl₂) and stored at -80°C until use.

[35 S]GTP γ S Binding. Binding assay was done on membranes prepared from CHO cells stably expressing FFA2. The optimum experimental conditions for the concentrations of GDP, MgCl₂, and NaCl in the assay buffer were initially determined. The assay was performed in assay buffer [20 mM HEPES, pH 7.5, 5 mM MgCl₂, and 0.1% (w/v) BSA] with 200 mM NaCl, 3 μ M GDP, and 5 μ g of membranes/well. The reaction was initiated by addition of 0.2 nM [35 S]GTP γ S in the absence or presence of various ligands and incubated at room temperature for 90 min. Nonspecific binding was determined in the presence of 100 μ M GTP γ S and was always less than 0.2% of total binding. Bound [35 S]GTP γ S was separated from free [35 S]GTP γ S by filtration through GF/B filters followed by five washes with 200 μ l of ice-cold assay buffer. Filter-bound radioactivity was determined by liquid scintillation counting.

Data Analysis. All results were presented as means \pm S.E.M. of separate experiments, each performed in duplicate. The concentration-dependent increases in FFA2 activation by ligands was expressed as a percentage increase above the basal unstimulated binding and analyzed by means of a nonlinear regression method using

the commercially available program Prism (GraphPad, San Diego, CA, with modifications suggested by Dr. Arthur Christopoulos) to produce the concentration eliciting half-maximal effect (EC_{50}) and the percentage maximal increase above the basal binding ($\%E_{max}$). The cooperativity factor and LogKB for allosteric modulation was calculated using the following allosteric global pEC_{50} equation: $\text{part1} = -1 \times \log(X + 10^{\text{LogKB}})$; $\text{part2} = \log(((10^{\text{Log}\alpha}) \times X) + (10^{\text{LogKB}}))$; $Y = \text{part1} + \text{part2} - \text{logd}$. The molar concentration of the modulator and pEC_{50} values (in the absence and presence of the allosteric modulator) are represented on the x - and y -axes, respectively.

Molecular Modeling. Sequence alignment and homology model were generated using PRIME (Jacobson et al., 2004) as implemented in Maestro (Maestro 8.5.110; Schrödinger, LLC, New York NY). The coordinates of the human β_2 -adrenergic receptor were used as template for model building (Cherezov et al., 2007). Side-chain and loop optimization was also performed using PRIME. Final model was energy minimized using MacroModel (version 9.6.1.1.0; Schrödinger, LLC) with OPLS-2001 force field (Kaminski et al., 2001). A harmonic constraint was applied to the TMs main chain with a force constant of 50 kcal/mol/Å. Flexible docking was performed using the Induce Fit Docking protocol as implemented in Maestro. Initial docking was done with GLIDE (Friesner et al., 2004) by using a receptor and ligand van der Waals scaling of 0.5. The top 20 poses were used as starting geometry for PRIME induce fit with a flexible zone defined by a radius of 5 Å around the ligand poses. Final ligand redocking and scoring was done with GLIDE XP. Each final complex was further optimized in MacroModel with OPLS-2005 force field (Kaminski et al., 2001) and GB/SA (Still et al., 1990) as continuum solvent effect using a dielectric constant of 1. Truncated Newton conjugated gradient (Ponder and Richards, 1987) with a convergence

threshold on the gradient of 0.05 KJ/Å/mol. During minimization, a 5-Å cavity within the ligand was allowed for free movement, and a harmonic constraint of 200 kcal/mol/Å was applied to atoms within 3 Å of the cavity. A final 3-Å frozen shell was include in the calculation, whereas the remaining residues were excluded. The ternary complexes were built from the respective binary receptor-ligand complexes, and the side chains were reoptimized with PRIME. The final geometry was optimized as described above.

Results

Identification of a Novel Synthetic Small Molecule Agonist for FFA2.

To identify novel synthetic ligands for FFA2 as tools to understand receptor function, we have carried out HTS against a chemical library consisting of more than 10^6 small-molecule compounds. Subsequent confirmation and follow-up analyses from HTS resulted in the identification of phenylacetamide 1 [(*S*)-2-(4-chlorophenyl)-3-methyl-*N*-(thiazol-2-yl)butanamide] as a novel and potent FFA2 agonist. Through initial structure activity relationship analysis, an analog, phenylacetamide 2 [(*S*)-2-(4-chlorophenyl)-*N*-(5-fluorothiazol-2-yl)-3-methylbutanamide], was also shown to have agonistic activity on FFA2. Both ligands showed specificity toward FFA2 and were inactive against a panel of GPCRs that included FFA1, FFA3, GPR109A, growth hormone secretagogue receptor, endothelin type B receptor, CCR2, CXCR3, CXCR4, and CCR7 at concentra-

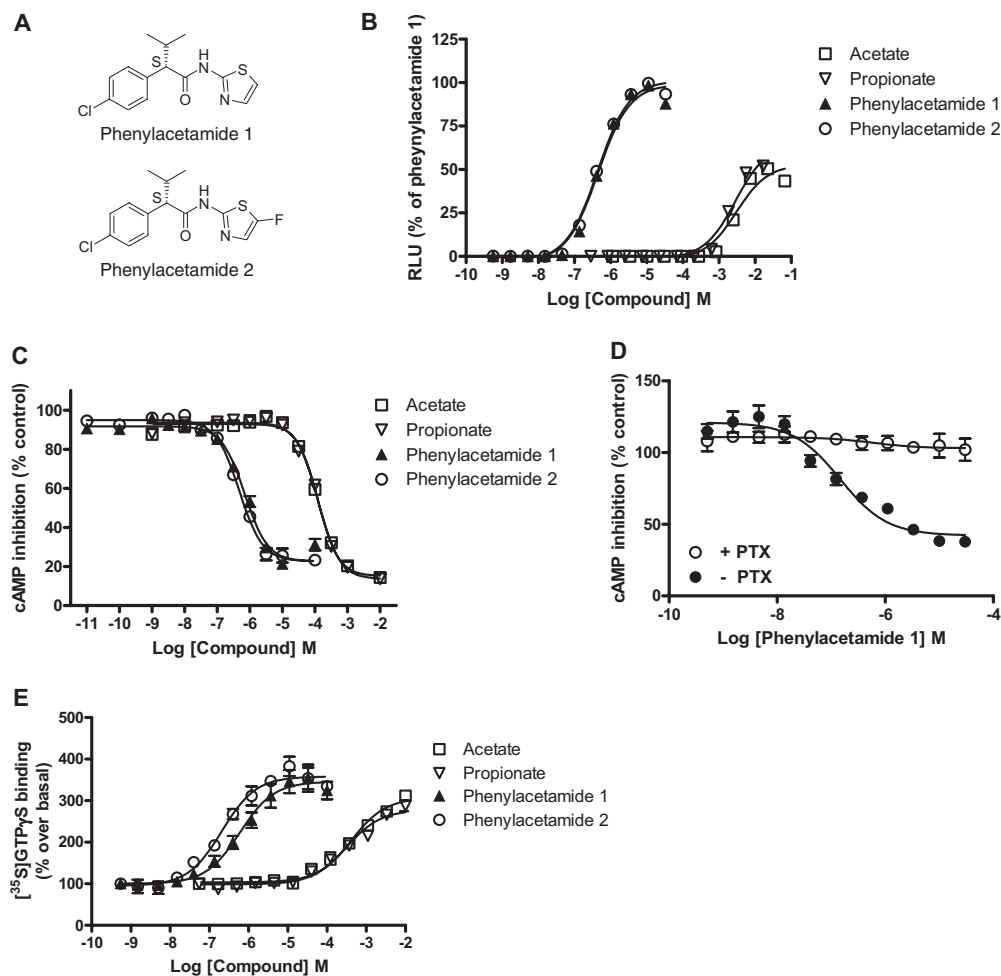


Fig. 1. Biological activity of phenylacetamides 1 and 2 in *in vitro* receptor functional assays. **A**, compound structures of phenylacetamides 1 and 2. **B**, response of Ca^{2+} release in CHO cells stably expressing hFFA2. Aequorin-mediated detection of Ca^{2+} release was measured. Data from four independent experiments were combined and normalized to percentage of phenylacetamide 2 maximum activity value. The average RLU measured for phenylacetamide 2 is 34,172,570. **C**, inhibition of cAMP response in CHO cells stably expressing hFFA2. Inhibition of forskolin-induced cAMP response was measured in the presence of different concentrations of ligands as indicated. Data from four independent experiments were combined and normalized to percentage of control (absence of ligand) expressed over concentration responses. The average basal RLU value measured was 25,280. **D**, PTX-sensitive response of phenylacetamide 1 in cAMP inhibition. Data are representative of three independent experiments, determined in duplicate. **E**, effect of FFA2 ligands on the binding of [35 S]GTP γ S to CHO membranes expressing FFA2 receptor. Binding of [35 S]GTP γ S was measured in the presence of different concentrations of ligands as indicated. Data are represented as percentage over basal activity (absence of the ligand) and are combined from three independent experiments. The average basal binding value corresponded to 0.14 to 0.19 pmol/mg protein. All data points were determined in duplicate.

tions up to 30 μM (data not shown). The chemical structures of phenylacetamides 1 and 2 are shown in Fig. 1A.

Because FFA2 has been reported to couple to both $\text{G}\alpha_i$ and $\text{G}\alpha_q$ pathways (Brown et al., 2003), the ability of phenylacetamides 1 and 2 to activate both pathways has been explored in $\text{G}\alpha_q$ -coupled aequorin and $\text{G}\alpha_i$ -coupled cAMP inhibition assays. Because CHO cells normally do not respond to the FFA2 endogenous ligands acetate and propionate, a CHO cell line stably expressing both human FFA2 (hFFA2) and aequorin was constructed to study the effects of various ligands on calcium mobilization by hFFA2 activation. In this cell line, the FFA2 endogenous ligands acetate and propionate as well as phenylacetamides 1 and 2 stimulated calcium mobilization in a concentration-dependent manner (Fig. 1B). Activation of calcium flux was independent of $\text{G}\alpha_i$, because pertussis toxin (PTX) treatment did not abolish calcium-dependent flash luminescence (data not shown). Phenylacetamides 1 and 2 both induced calcium mobilization with higher efficacy than acetate and propionate in the aequorin assay. Phenylacetamides 1 and 2 have similar potency, with EC_{50} values of 0.45 and 0.44 μM against hFFA2, respectively, and were much more potent than acetate and propionate in this assay (Fig. 1B and Table 1).

The effects of FFA2 ligands on $\text{G}\alpha_i$ -mediated signaling pathway were also studied in the CHO cell line stably expressing FFA2. Similar to previous reports, acetate and propionate inhibited the forskolin-induced cAMP response with IC_{50} values in the range of 120 to 140 μM against both the human and mouse receptors (Fig. 1C and Table 1). Both phenylacetamides 1 and 2 were significantly more potent than endogenous ligands against human and mouse FFA2, with IC_{50} values in the ranges of 0.7 to 0.96 μM and 0.48 to 0.66 μM , respectively (Fig. 1C and Table 1). No significant potency difference was detected between human and mouse receptors in CHO cells stably expressing these receptors (Table 1). The observed inhibition of forskolin-induced cAMP response was a direct consequence of $\text{G}\alpha_i$ -mediated signaling, as this effect was abolished in the presence of PTX (Fig. 1D).

The effects of the synthetic ligands on FFA2 function were further explored in the stimulation of [^{35}S]GTP γS binding to hFFA2. The FFA2 endogenous ligands acetate and propionate stimulated [^{35}S]GTP γS binding in membranes prepared from CHO cells stably expressing hFFA2 in a concentration-dependent manner. The maximal agonist stimulation was observed at approximately 3 mM, corresponding to approximately 3-fold increases from the basal activity measured in the absence of the agonist (Fig. 1E). Activation of G protein through FFA2 was also observed with the synthetic ligands (phenylacetamides 1 and 2), with a stimulation of 3- to 3.5-fold over basal and a slightly higher efficacy than

endogenous ligands (Fig. 1E). Agonist-induced [^{35}S]GTP γS binding was abolished upon PTX treatment and was not detected from membrane preparations from parental CHO cells, indicating that the effects are indeed mediated through FFA2 coupling to $\text{G}\alpha_i$ pathway (data not shown). Therefore, based on the results in Fig. 1, we concluded that phenylacetamides 1 and 2 are agonists for FFA2 and are capable of activating both $\text{G}\alpha_q$ - and $\text{G}\alpha_i$ -coupled pathways for receptor function.

Phenylacetamides 1 and 2 Activate $\text{G}\alpha_i$ Pathway and Inhibit Lipolysis in Adipocytes. We have shown previously that activation of FFA2 by endogenous ligands in adipocytes could lead to the inhibition of lipolysis (Ge et al., 2008). This effect is similar to that observed for another adipocyte-expressed receptor, GPR109A. Activation of GPR109A by its ligand, nicotinic acid, mediated through $\text{G}\alpha_i$ pathway, led to the inhibition of lipolysis (Wise et al., 2003, Tunaru et al., 2003, Soga et al., 2003). Given that the synthetic ligands behaved similarly to endogenous ligands in $\text{G}\alpha_q$ and $\text{G}\alpha_i$ mediated assays but with higher potency, we examined the effects of these synthetic ligands on lipolysis in adipocytes. Phenylacetamides 1 and 2 both inhibited lipolysis in 3T3L1 adipocytes in a concentration-dependent manner as measured by the reduction of glycerol production in the media (Fig. 2). Such inhibition was sensitive to PTX treatment, indicating that this was the result of activating the $\text{G}\alpha_i$ -coupled signaling pathway, similar to our previously reported effects of acetate and propionate on FFA2 in adipocytes (Ge et al., 2008).

Phenylacetamides 1 and 2 Are Allosteric Agonists for FFA2. Although both endogenous and synthetic ligands behave as agonists in FFA2-mediated activity assays as shown in Fig. 1, given the differences in the chemical structures of these ligands, we were interested in finding whether these effects were mediated through ligand binding to the same or different sites on the receptor. To address this question, various combinations of ligand treatments in the different assays described below were carried out.

The first indication that phenylacetamides 1 and 2 have allosteric effects relative to acetate and propionate came from analysis in forskolin-induced cAMP assays. As shown in Fig. 3A, acetate concentration-dependently inhibited forskolin induced cAMP production. The effects of propionate on the acetate concentration response resulted in a decrease in basal cAMP levels without affecting the potency of acetate (Fig. 3A). The decrease in the basal cAMP level is due to the activity of propionate alone on the receptor, and the lack of a shift in potency on acetate upon addition of propionate suggested that propionate and acetate bind to the same or overlapping sites on the receptor. Similar biochemical effects

TABLE 1

Summary of FFA2 potencies

Data are average $\text{IC}_{50}/\text{EC}_{50}$ values \pm standard error (S.E.) from four independent experiments.

Ligand	hFFA2		mFFA2	
	cAMP (IC_{50})	Aequorin (EC_{50})	cAMP (IC_{50})	Aequorin (EC_{50})
	μM			
Acetate	123.8 \pm 9.2	3032 \pm 1083	131.0 \pm 9.7	1153 \pm 159.4
Propionate	125.2 \pm 9.9	2862 \pm 988	120.2 \pm 10.7	709.7 \pm 99.5
Phenylacetamide 1	0.70 \pm 0.07	0.45 \pm 0.07	0.96 \pm 0.07	1.27 \pm 0.10
Phenylacetamide 2	0.48 \pm 0.04	0.44 \pm 0.07	0.66 \pm 0.07	0.62 \pm 0.06

were also observed between phenylacetamides 1 and 2. The addition of phenylacetamide 2 to phenylacetamide 1 concentration responses compared with that of phenylacetamide 1 alone resulted in the suppression of basal cAMP levels without changing the potency of phenylacetamide 1, suggesting that these two synthetic ligands are binding to the same or overlapping sites on the receptor (Fig. 3B). However, different results were achieved when endogenous ligands and synthetic ligands were combined. When phenylacetamide 1 was added to acetate concentration-response studies, not only was there suppression in the basal cAMP levels, but there was also a significant left shift in the acetate concentration responses (Fig. 3C). The reverse also holds true: the addition of acetate significantly left-shifted phenylacetamide 1 concentration responses (Fig. 3D). Therefore, if the binding site for endogenous ligands is defined as an orthosteric site, then these data suggest that phenylacetamides 1 and 2 bind to allosteric site on the receptor and induce positive cooperativity with acetate or propionate. The cooperativity factor (α) for phenylacetamide 1 on acetate is 24 ($\text{Log}\alpha = 1.38$) in the $\text{G}\alpha_i$ -mediated cAMP inhibition assay (Table 2).

To determine whether this positive allosteric effect could also occur in $\text{G}\alpha_q$ signaling, concentration response curves were generated from various combinations of endogenous ligands and synthetic ligands in aequorin assays measuring calcium fluxes induced by activation of $\text{G}\alpha_q$ pathway by FFA2. The results show that the potency of acetate was increased in the presence of phenylacetamide 1 with a cooperativity factor of 89 ($\text{Log}\alpha = 1.95$; Fig. 4A). In a reciprocal experiment, acetate increased the potency of phenylacetamide 1 with a cooperativity factor of 24 ($\text{Log}\alpha = 1.38$; Fig. 4B). On the other hand, phenylacetamide 2 did not allosterically modulate the FFA2 receptor at any concentration of phenylacetamide 1 (Fig. 4C). These results suggest that phenylacetamide 1 can positively modulate acetate activity in $\text{G}\alpha_q$ -mediated receptor signaling in addition to $\text{G}\alpha_i$ pathway.

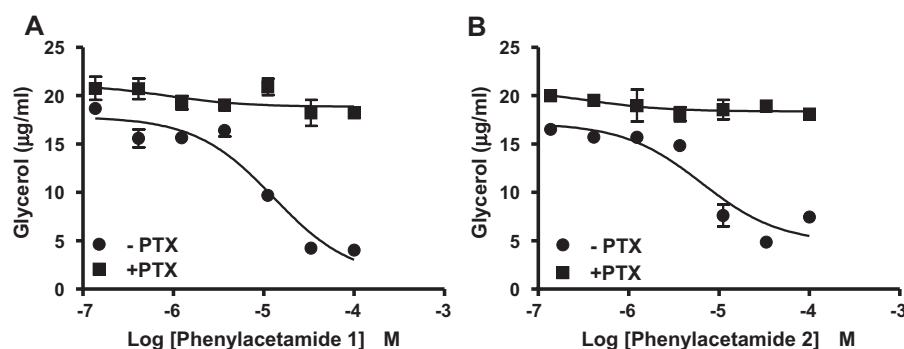


Fig. 2. The synthetic ligands phenylacetamide 1 and 2, inhibit lipolysis in adipocytes. Differentiated 3T3L1 cells were treated with phenylacetamide 1 (A) or 2 (B) in the presence or absence of PTX. Lipolysis was measured by the release of glycerol in the culture medium. Data are representative of three independent experiments, determined in duplicate.

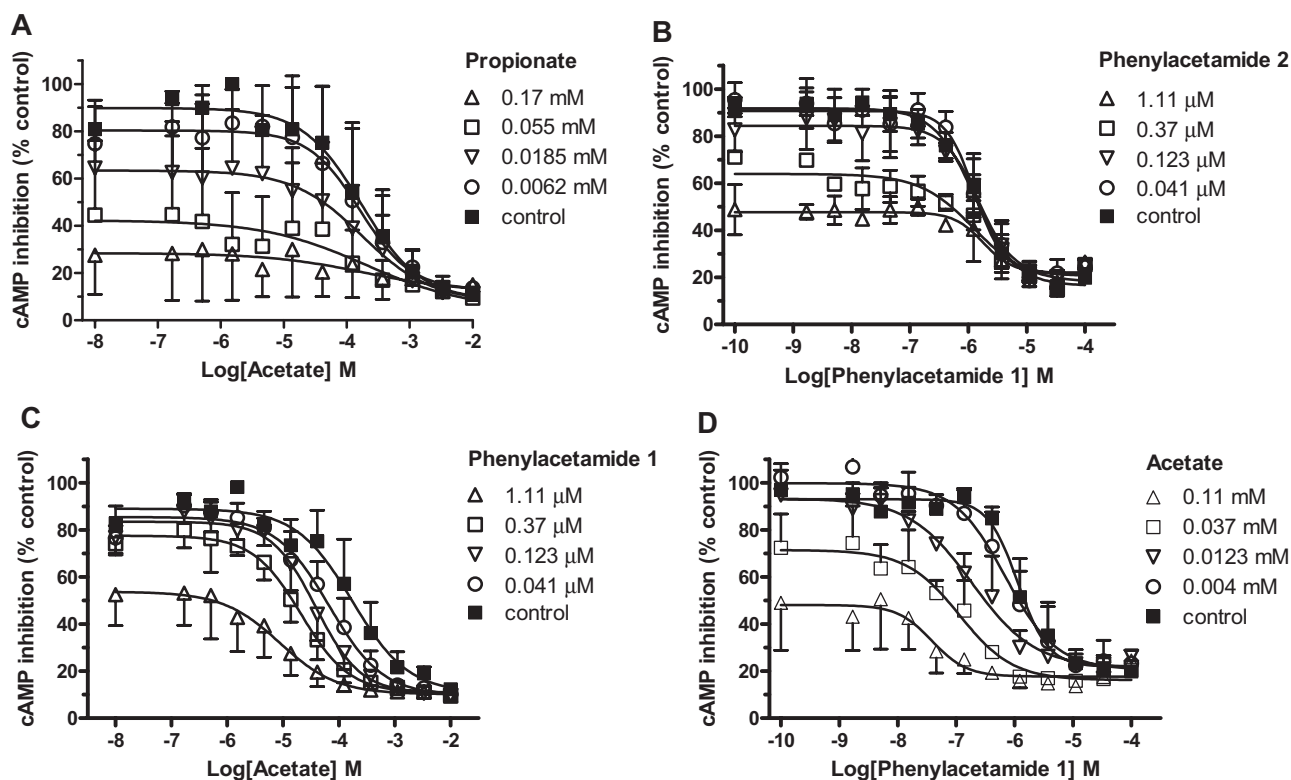


Fig. 3. Allosteric activity of phenylacetamides 1 and 2 in cAMP assays. Inhibition of forskolin-induced cAMP response was measured in the presence of different concentrations of agonists: acetate versus propionate (A), phenylacetamide 1 versus 2 (B), acetate versus phenylacetamide 1 (C), and phenylacetamide 1 versus acetate (D). Data were combined from three independent experiments and expressed as percentage of no ligand control. The average basal RLU measured was 27,570.

concentration-response curve of either phenylacetamide 1 or phenylacetamide 2 in the presence of fixed concentrations of acetate and propionate (0.0135–10 mM). There was a significant left shift in the potency of phenylacetamides 1 and 2 in the presence of the endogenous ligands with a cooperativity factor of 10 (Table 3). On the other hand, phenylacetamide 1 did not allosterically modulate the FFA2 receptor in stimulating [35 S]GTP γ S binding at any concentration of phenylacetamide 2. Likewise, no positive cooperativity was observed with acetate in the presence of propionate on FFA2 in the GTP γ S binding assay (data not shown). These results further support the conclusion that the synthetic ligands, phenylacetamides 1 and 2, interact allosterically at the FFA2 receptor through a site distinct from that of the endogenous ligands.

Molecular Modeling of Ligand Binding to FFA2. To gain further insights into the observed positive cooperativity between endogenous and synthetic ligands, a molecular model has been built for FFA2 by homology modeling using the X-ray crystal structure of the human β_2 -adrenergic receptor as a template (Cherezov et al., 2007). The side chains and the extracellular loops were further optimized using PRIME (Jacobson et al., 2004) as described under *Materials and Methods*. Although potential amino acid residues in-

The logK_B values and cooperativity factors of the ligands are calculated by fitting the data to allosteric global pIC₅₀ equation (see *Materials and Methods*). Data represented is mean ± S.E. from three independent experiments performed in duplicate.

Ligands	Log K _B	Log α (Cooperativity Factor)
Acetate + phenylacetamide 1	-6.0 \pm 0.14	1.38 \pm 0.11
Phenylacetamide 1 + acetate	-3.5 \pm 0.91	1.95 \pm 0.91
Phenylacetamide 1 + phenylacetamide 2	-7.05 \pm 0.07	-0.10 \pm 0.15
Acetate + propionate	-5.7 \pm 1.1	0.3 \pm 0.04

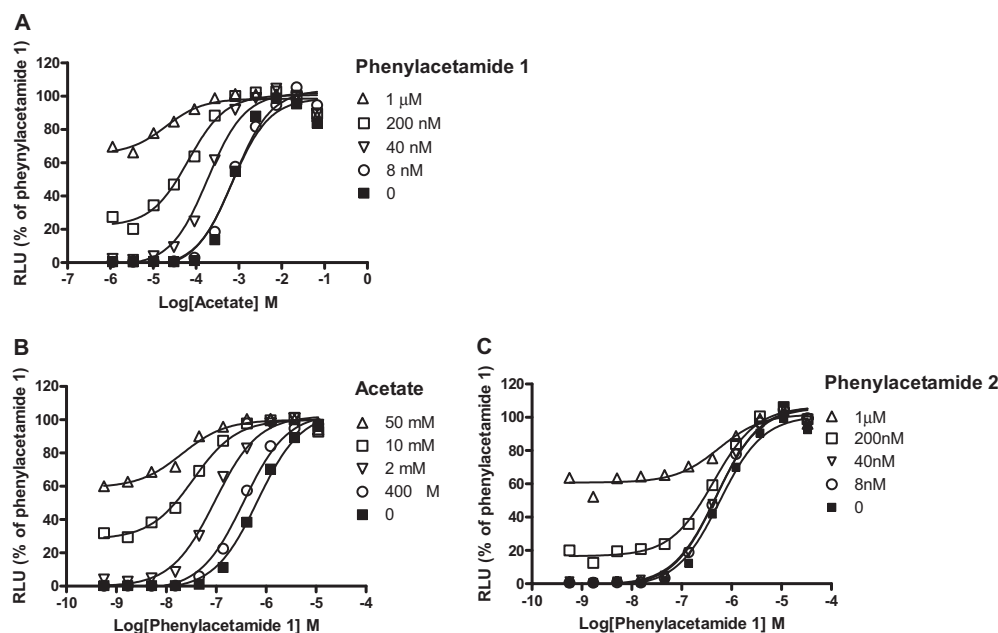


Fig. 4. Allosteric modulation of acetate by phenylacetamide 1 in aequorin assay. A, the allosteric effect of phenylacetamide 1 on acetate-induced calcium flux. B, the positive cooperating effect of acetate on phenylacetamide 1-induced calcium flux. C, the lack of cooperating effect of phenylacetamide 2 on phenylacetamide 1-induced calcium flux. Data were derived from two independent experiments and normalized to percentage of the maximal response from phenylacetamide 1 with an average RLU of 35,896,085.

involved in FFA2 ligand binding sites are currently unknown, regions and residues that might be important for FFA2 ligand recognition could be suggested based on the recently

identified residues that are important for FFA1 ligand recognition (Sum et al., 2007) and the conservation between FFA1 and FFA2 (Fig. 7A). By sequence comparison with FFA1, we focused our efforts in particular in the regions containing Arg180 in TM5, Arg255 in TM7, and His242 in TM6. An area of approximately 10 Å around these residues was used for ligand docking with flexibility for all the side chains contained within the region as well as loops of the main chain. The endogenous ligands acetate and propionate as well as phenylacetamide 1 were individually docked using this procedure, and multiple docking poses were selected for further analysis. The emphasis was then put on putative binding sites with little or no overlap between acetate or propionate and phenylacetamide 1. After this analysis, one potential binding mode for the SCFAs and two potential binding sites for phenylacetamide 1 were selected for further evaluation (Fig. 7B).

Flexible docking and energy minimization results for acetate and propionate showed a binding mode in which the acid functionality was interacting with both the Arg180 and Arg255 (Fig. 7C). The negatively charged carboxylate interacts with both arginine residues in a bi-dentate like fashion. The aliphatic chain is oriented toward a shallow hydrophobic pocket made of residues from TM6 and TM7. The residues in contact with the hydrophobic moiety of the endogenous ligand include Ser241, Tyr238, and the hydrophobic portions of Lys250 and Arg255. Although we did not model all the SCFAs, the cavity size and proximity of some of these residues to the γ carbon of the propionate suggest that binding of four carbon chain analog could have some steric repulsion especially from Tyr238. Moreover, this cavity will not be able to accommodate FFAs with 5 or more atoms without major conformational changes, which in turn could yield high-energy and unfavorable complexes and, therefore, could potentially explain the preference of FFA2 for SCFA (Le Poul et al., 2003).

Flexible docking and minimization yielded two possible binding sites for phenylacetamide 1. A putative binding mode 1 is located in a cavity between TM2, TM3, TM6, and TM7. In this binding mode, the hydrophobic *p*-chloro phenyl of phenylacetamide 1 is oriented toward the interior of the transmembrane region, making several hydrophobic contacts. In addition, the isopropyl group of phenylacetamide 1 is also located in a hydrophobic environment. The amide thiazole moiety, on the other hand, is oriented toward the extracellular loops, showing potential polar contacts from the amide carbonyl with the backbone NH of Leu173 (Fig. 7D), although the donor-acceptor angle is not ideal for a strong hydrogen bond. In this binding mode, Arg255 is in close contact with phenylacetamide 1, forming a possible stacking interaction

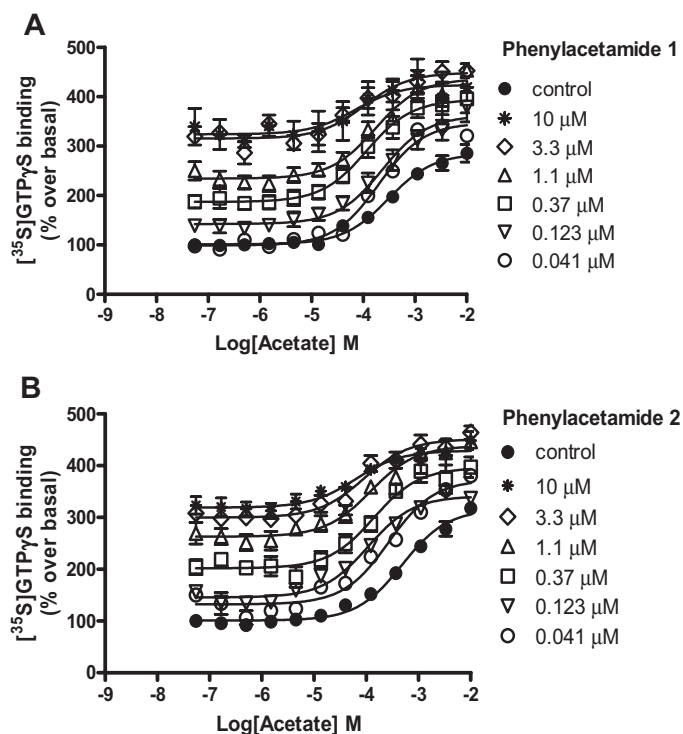


Fig. 5. Allosteric modulation of acetate by phenylacetamides 1 and 2 in GTP γ S binding assay. The allosteric effects of phenylacetamides 1 (A) and 2 (B) on acetate in the stimulation of [35 S]GTP γ S binding were determined. Data were combined from three independent experiments performed in duplicate and were expressed as percentage of control (in the absence of ligand). The average control values measured corresponded to 0.14 to 0.19 pmol/mg protein.

TABLE 3

Stimulation of [35 S]GTP γ S binding by FFA2 agonists in the presence of different concentrations of allosteric ligands on FFA2 receptor

The log K_B values and cooperativity factors of the ligands are calculated by fitting the data to allosteric global pEC $_{50}$ equation (see *Materials and Methods*). Data represented is mean \pm S.E.M. from two to three independent experiments performed in duplicate.

Ligands	Log K_B	Log α (Cooperativity Factor)
Acetate + phenylacetamide 1	-6.38 ± 0.73	0.72 ± 0.03
Acetate + phenylacetamide 2	-6.2 ± 0.39	1.0 ± 0.133
Propionate + phenylacetamide 1	-6.0 ± 0.66	1.1 ± 0.27
Propionate + phenylacetamide 2	-6.67 ± 0.90	0.6 ± 0.07
Phenylacetamide 1 + acetate	-3.5 ± 0.37	1.14 ± 0.3
Phenylacetamide 2 + acetate	-3.0 ± 0.05	1.13 ± 0.08
Phenylacetamide 1 + propionate	-3.5 ± 0.14	0.97 ± 0.02
Phenylacetamide 2 + propionate	-3.3 ± 0.57	1.2 ± 0.08

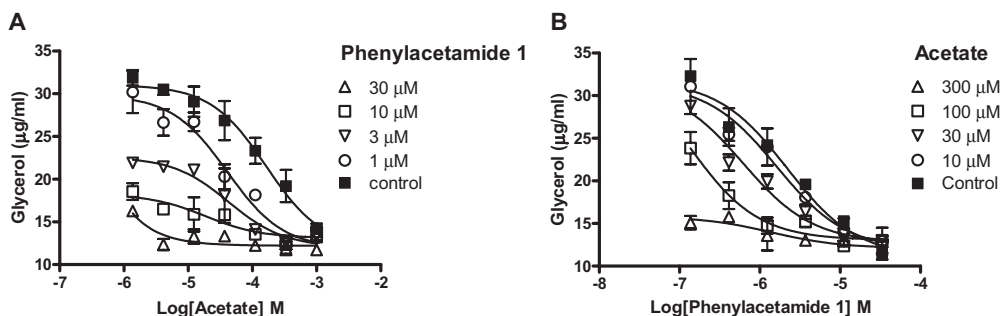


Fig. 6. Allosteric modulation of acetate by phenylacetamide 1 in lipolysis assay. Differentiated 3T3L1 cells were treated with acetate concentration response at fixed concentrations of phenylacetamide 1 (A) or with phenylacetamide 1 concentration response at fixed concentrations of acetate (B). Lipolysis was measured by the release of glycerol in the culture medium. Data are representative of three independent experiments, determined in duplicate.

with the thiazole moiety. Arg255 is also involved in H-bond interaction with the carbonyl backbone of Leu173. We hypothesize that these interactions help to stabilize the complex with phenylacetamide 1 by holding the Leu173 side chain in tight contact with the *p*-chloro-phenyl ring, hence improving the hydrophobic interactions. The second binding mode identified by flexible docking is located in a cavity between TM3, TM5, and TM6 (Fig. 7E). In this orientation, the entire ligand is buried in the transmembrane region. The *p*-chloro phenyl group of phenylacetamide 1 is surrounded by hydrophobic residues, whereas the thiazole amide is proximal to His242, making a hydrogen bond interaction with the NH of the side chain. In principle, both binding modes for phenylacetamide 1 could potentially explain the allosterism, because there is no overlap with the proposed binding site for the SCFAs. However, to have positive cooperative effect, not only should the binding mode for phenylacetamide 1 not overlap with the binding of SCFAs, but also the hypothetical ternary complex formed should have improved intermolecular interactions compared with the corresponding binary states. A comparison between the complexes with phenylacetamide 1, in binding mode 1, and propionate shows smaller variations on the surrounded side chains. In contrast, the geometry of the complex for phenylacetamide 1 in binding mode 2 showed a significant shift of Arg180 and His242 compared with the complex with propionate. This shift is necessary for accommodating the synthetic ligand and could have a negative impact on the formation of a stable ternary complex. Therefore, binding mode 1 seems to be more suitable for explaining the allosteric synergism observed between the endogenous ligands and phenylacetamide 1 series.

To explain the selectivity of phenylacetamide 1 and phenylacetamide 2 over FFA3, we examined the residues lining the potential binding mode 1 in the modeled FFA2 structure and identified several residues in close contact with the ligand that are different between the two FFA receptors. These residues include Ile66 and Ser256, which are replaced by Met62 and Ile252, respectively, in FFA3. The significant size and property differences of these FFA3 residues could cause significant steric hindrance and contribute to the observed selectivity. In addition, Asp170 in FFA2 is replaced by Ala170 in FFA3, which breaks a potential intramolecular H-bond in the EL2 loop that is involved in the binding of phenylacetamide 1. These potential differences in the binding pocket are shown in Fig. 7F, where the FFA2 residues have been mutated to the corresponding FFA3 residues to highlight the potential steric hindrance.

The hypothetical ternary complex using binding mode 1 for phenylacetamide 1 and the binding site identified for propionate is shown in Fig. 7G. A model for this ternary complex was obtained by merging the individual ligands into their respective binding sites followed by geometry optimization for residues in a 7-Å radius around each ligand. In this complex, propionate has similar bi-dentate salt bridge interaction as in the binary complex. In addition, the interaction of the amide carbonyl oxygen of phenylacetamide 1 with the backbone NH of Leu173 has a much better geometry for a hydrogen bond than in the corresponding binary complex because of the displacement of Arg255 toward the propionate. Furthermore, the thiazole amide moiety rotates around 90° relative to the binary complex, and this further enhances the H-bond interaction. Based on these rearrange-

ments around the ligand binding site, we hypothesize that the thiazole amide moiety of phenylacetamide 1 helps to better orient the side chain of Arg255 toward the propionate ion by inserting between the extracellular loop 2 (EL2) and the phase of Arg255 side chain. At the same time, the presence of the SCFA attracts Arg255, allowing a better hydrogen-bond interaction for phenylacetamide 1. Overall, these effects should bring more stability to the ternary complexes, which could result in a corresponding positive cooperative effect.

Discussion

Acetate and propionate have previously been identified as endogenous ligands for FFA2 (Brown et al., 2003). However, no potent synthetic small molecule ligands specific for FFA2 have been reported. In this report, we describe the identification and characterization of two phenylacetamide derivatives, phenylacetamides 1 and 2, as novel synthetic allosteric agonists for FFA2. Similar to the activities of endogenous ligands, the synthetic ligands can induce FFA2 coupling to both G_{α_i} and G_{α_q} signaling pathways in multiple assay formats (Fig. 1). In addition to the greatly improved potency of the synthetic ligands over the endogenous ligands, the synthetic ligands show higher efficacy than acetate and propionate in G_{α_q} -coupled aequorin assay (Fig. 1B) and slightly increased efficacy in more G_{α_i} -coupled [35 S]GTP γ S binding assays (Fig. 1E). The differences in efficacy between endogenous and synthetic ligands in different assays could be the result of differences in coupling efficiencies of G_{α_i} versus G_{α_q} subunits to FFA2 for the two distinct classes of ligands. The synthetic ligands also activated the receptor in its native setting by inhibiting lipolysis in adipocytes via G_{α_i} -dependent pathway similar to what has been described for endogenous ligands (Ge et al., 2008). All of these results strongly

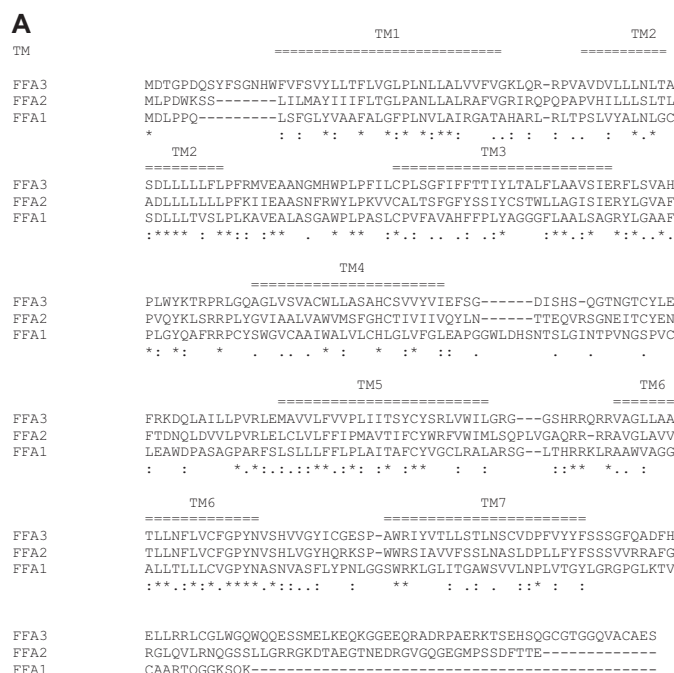


Fig. 7. Molecular modeling of ligand binding on FFA2. A, sequence alignment for FFA1, FFA2, and FFA3.

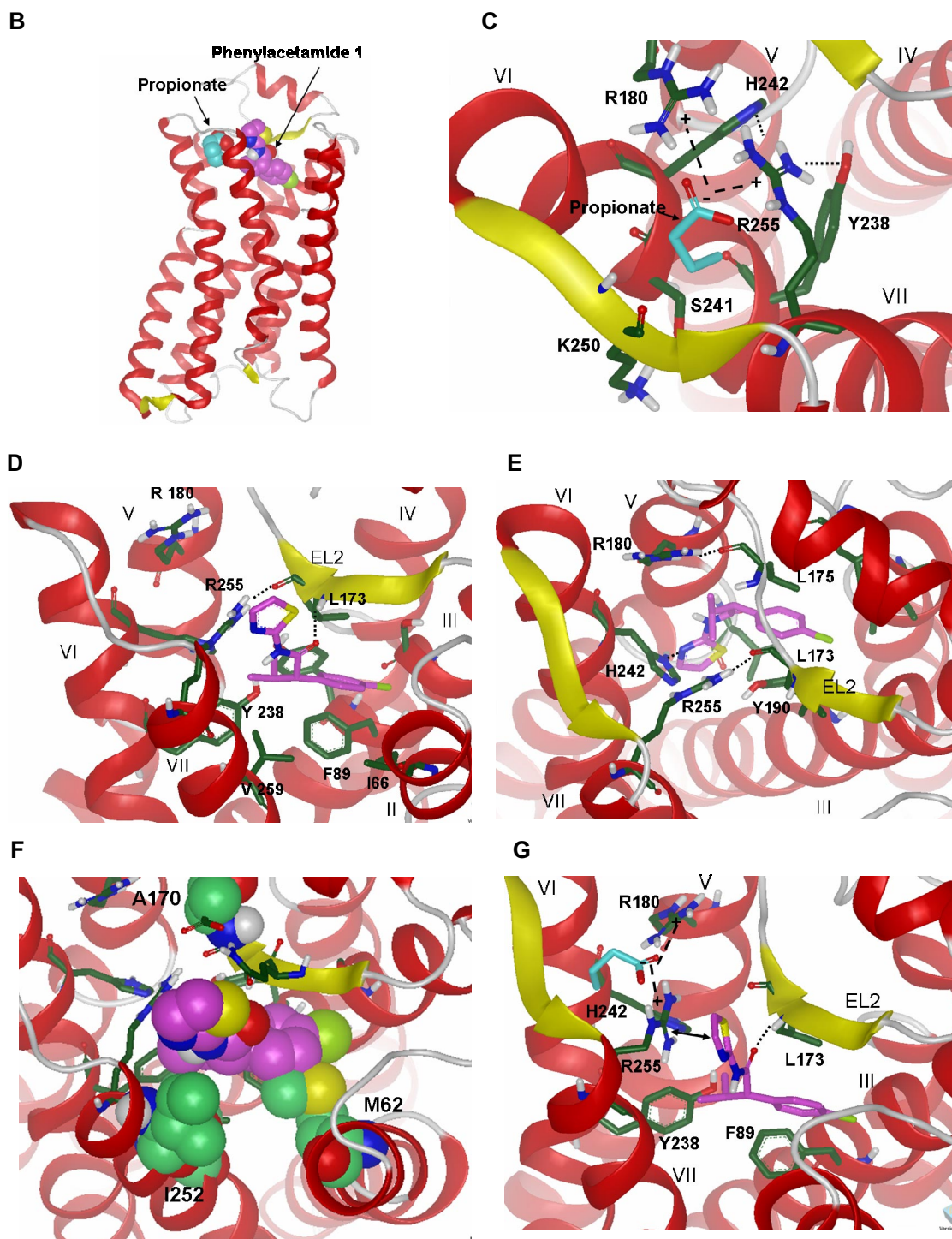


Fig. 7. (continued) B, model of the human FFA2 and putative binding sites for endogenous ligand propionate (cyan) and allosteric synthetic agonist phenylacetamide 1 (magenta). Both ligands are in close proximity but do not share the same binding site. C, putative binding mode for propionate (cyan). Salt bridge interactions between the carboxylate anion of the ligand and guanidinium cation groups of Arg180 and Arg255 are shown in dashed lines. Lipophilic chain is in a gauche conformation and oriented toward Ser241 and between Arg255 and Lys250 side chains. Additional intramolecular H-bond interactions between Arg255, His242, and Tyr238 help to stabilize the complex. D, putative binding mode 1 for synthetic agonist phenylacetamide 1 (magenta). Hydrogen bond interactions between the Leu173 backbone and phenylacetamide 1 as well as the guanidinium cation group of Arg255 are shown in dotted lines. The lipophilic *p*-chlorophenyl group is surrounded by several hydrophobic residues, shown in green, from TM2 (Ile66), TM3 (Phe89), TM6 (Tyr238), TM7 (Val259), and the EL2 loop (Leu173). E, putative binding mode 2 for synthetic agonist phenylacetamide 1 (magenta). Hydrogen-bond interactions are shown in dotted lines. F, putative binding mode 1 for synthetic agonist phenylacetamide 1 (magenta). The lipophilic *p*-chlorophenyl group is surrounded by several hydrophobic residues. In Corey-Pauling-Koltun representation, light blue is shown the corresponding different residues in FFA3. Met62 and to some extent Ile252 of FFA3 show overlaps with the ligand binding that may cause significant steric hindrance. G, model for a ternary complex of the endogenous ligand propionate (cyan) and synthetic agonist phenylacetamide 1 (magenta). Hydrogen bond interactions between the Leu173 backbone and phenylacetamide 1 is shown as a dotted line. Salt bridge interactions between propionate and conserved arginine residues are shown as dashed lines. The packing interaction between phenylacetamide 1 and Arg255 is also indicated.

support the conclusion that the synthetic ligands are agonists for FFA2.

To gain more insight into how these endogenous and synthetic ligands activate the receptor, we carried out various experiments using different combinations and concentration of ligands. It was interesting to note that the endogenous and synthetic ligands showed positive cooperativity with each other in either upstream or downstream pathways. We observed a greater degree of cooperativity in cAMP assay and aequorin assay, which may be due to amplification of the response through the receptor compared with [³⁵S]GTPγS binding assays. A positive allosteric effect is defined by a cooperativity factor of greater than 1 ($\alpha > 1$) (Christopoulos and Kenakin, 2002; Langmead and Christopoulos, 2006). Phenylacetamide 1 significantly potentiated (24–89-fold, $\text{Log } \alpha = 1.38\text{--}1.95$) the functional potency of orthosteric ligand acetate to FFA2 in cAMP inhibition and Ca^{2+} stimulation assays. This positive cooperativity would not be observed from ligands binding to the same site on the receptor. Indeed, in the inhibition of forskolin-induced cAMP assay, the addition of propionate did not affect the potency of acetate concentration responses; rather, only the baseline was reduced as a result of the activity of propionate alone in the assay (Fig. 3). A similar relationship was observed between phenylacetamides 1 and 2, suggesting that ligands of each class share similar binding sites on the receptor (Fig. 3). A more definitive method to study whether ligands have overlapping binding sites on a receptor is to use radiolabeled ligands, which have been used extensively to study allosterism on other GPCRs (Tränkle et al., 2003, 2005; Prilla et al., 2006). Although the potency of our synthetic ligands does not allow the development of a radioligand binding assay to directly measure binding sites on the receptor, these results still strongly support the conclusion that synthetic ligands bind to an allosteric site on the receptor and that they show positive cooperativity with endogenous ligands, similar to allosteric modulators reported in other GPCRs, including calcium sensing receptor (Nemeth et al., 2004), A1 adenosine receptor (Kollias-Baker et al., 1997), metabotropic glutamate receptor (Hemstapat et al., 2006), and others (May et al., 2007).

Such positive cooperativity was also observed in a native cell line. We and others have previously shown that activation of FFA2 in adipocytes by endogenous ligands, acetate and propionate, results in the inhibition of lipolysis via $\text{G}\alpha_i$ signaling pathway (Hong et al., 2005; Ge et al., 2008). In this adipocyte lipolysis assay, phenylacetamide 1, in addition to being an FFA2 agonist, also showed positive cooperativity to acetate. The addition of phenylacetamide 1 resulted in a significant left shift in acetate concentration response curve, and the reciprocal combination also generated similar cooperativity (Fig. 6). These results suggest that the observed allosteric effects of synthetic ligands are not in vitro assay artifacts but could have significance in receptor function in a more physiological setting.

To further understand the nature of allosteric interaction between endogenous and synthetic ligands, a molecular model was built for FFA2 by homology modeling using the X-ray crystal structure of the human β_2 -adrenergic receptor (Cherezov et al., 2007) as a template. Based on the identified residues that are important for FFA1 ligand interaction and the homology between FFA1 and FFA2, putative ligand bind-

ing pockets for endogenous ligands and the synthetic ligands were identified (Fig. 7). Analysis of the optimized ternary complex between receptor, propionate, and phenylacetamide 1, highlighted a number of important residues that could influence the binding of these two classes of ligands and provided a possible explanation for the observed positive cooperativity. However, this model needs to be verified experimentally and could be tested by site-directed mutagenesis of the residues identified. Therefore, on the basis of the sequence alignment and molecular modeling described here, Arg180 and Arg255 could be selected to explore their roles in binding with the carboxylate group of the SCFAs, and Ile66, Phe89, Leu173, Tyr238, and Val259 could be selected to explore their involvement in hydrophobic interactions with phenylacetamide 1, as suggested in the proposed binding mode 1.

Allosteric agonists have been known to affect signaling in their own right, which opens new avenues in understanding receptor structure, pharmacology and physiological function. Positive allosteric agonists offer an attractive therapeutic approach for the activation of GPCRs because they would be efficacious in the presence or absence of endogenous agonist, and they might elicit less tachyphylaxis and/or receptor desensitization than competitive agonists (Langmead and Christopoulos, 2006). They could also potentially offer greater selectivity on the receptor by binding to a nonconserved region on the receptor from a family of related receptors and provide a greater magnitude of physiological response (May et al., 2007).

The identification of a novel allosteric site on FFA2 for the first time is of great importance in understanding FFA2 physiological functions. The presence of this allosteric site on the FFA2 receptor can be used to explore and develop new compounds with greater efficacy and potency that selectively target diseases related to this receptor. Furthermore, the allosteric site provided the platform for the identification of FFA2 selective ligands over related subfamily members such as FFA3, which is also a SCFA receptor. However, a potential cooperative effect of any novel synthetic ligands with either endogenous ligands or substances that could be converted to acetate or propionate should be a particularly important consideration for future in vivo pharmacology study designs. For example, the primary fate of ethanol metabolism by the liver is the conversion and release of acetate into circulation. Plasma levels of acetate could increase up to 20-fold and into millimolar concentrations after alcohol ingestion (Lundquist et al., 1962; Siler et al., 1999). Therefore, the use of ethanol as vehicle in animal model studies, or the administration of a drug against FFA2 in humans, with or without alcohol consumption, could potentially alter the effects and outcome of any studies using FFA2. In conclusion, we have identified novel synthetic allosteric agonists for FFA2; these and potentially other allosteric agonists represent a new and exciting avenue for research and possible therapeutic intervention on FFA2.

Acknowledgments

We thank Qi Guo, Yi-Shan Chou, and Zhongyu Wang for technical support. We thank Xiaoning Zhao, Richard Lindberg, Wen-Chen Yeh, Bei Shan, Ulrike Schindler, Nigel Walker, Jin-Long Chen, Randall Hungate, William Simonet, and David Lacey for helpful discussions and critical reading of the manuscript.

References

- An S, Bleu T, Zheng Y, and Goetzl EJ (1998) Recombinant human G protein-coupled lysophosphatidic acid receptors mediate intracellular calcium mobilization. *Mol Pharmacol* **54**:881–888.
- Brown AJ, Goldsworthy SM, Barnes AA, Eilert MM, Tcheang L, Daniels D, Muir AI, Wigglesworth MJ, Kinghorn I, Fraser NJ, et al. (2003) The Orphan G protein-coupled receptors GPR41 and GPR43 are activated by propionate and other short chain carboxylic acids. *J Biol Chem* **278**:11312–11319.
- Carlson LA (2005) Nicotinic acid: the broad-spectrum lipid drug. A 50th anniversary review. *J Intern Med* **258**:94–114.
- Cherezov V, Rosenbaum DM, Hanson MA, Rasmussen SG, Thian FS, Kobilka TS, Choi HJ, Kuhn P, Weis WI, Kobilka BK, et al. (2007) High-resolution crystal structure of an engineered human beta2-adrenergic G protein-coupled receptor. *Science* **318**:1258–1265.
- Christopoulos A and Kenakin T (2002) G protein-coupled receptor allostery and complexing. *Pharmacol Rev* **54**:323–374.
- Covington DK, Briscoe CA, Brown AJ, and Jayawickreme CK (2006) The G-protein-coupled receptor 40 family (GPR40-GPR43) and its role in nutrient sensing. *Biochem Soc Trans* **34**:770–773.
- Fredriksson R, Lagerström MC, Lundin LG, and Schiöth HB (2003) The G-protein-coupled receptors in the human genome form five main families. Phylogenetic analysis, paralogon groups, and fingerprints. *Mol Pharmacol* **63**:1256–1272.
- Fredriksson R and Schiöth HB (2005) The repertoire of G-protein-coupled receptors in fully sequenced genomes. *Mol Pharmacol* **67**:1414–1425.
- Friesner RA, Banks JL, Murphy RB, Halgren TA, Klicic JJ, Mainz DT, Repasky MP, Knoll EH, Shelley M, Perry JK, et al. (2004) Glide: a new approach for rapid, accurate docking and scoring. 1. Method and assessment of docking accuracy. *J Med Chem* **47**:1739–1749.
- Ge H, Li X, Weiszmann J, Wang P, Baribault H, Chen JL, Tian H, and Li Y (2008) Activation of GPR43 in adipocytes leads to inhibition of lipolysis and suppression of plasma free fatty acids. *Endocrinology* **149**:4519–4526.
- Hemstapat K, de Paulis T, Chen Y, Brady AE, Grover VK, Alagille D, Tamagnan GD, and Conn PJ (2006) A novel class of positive allosteric modulators of metabotropic glutamate receptor subtype 1 interact with a site distinct from that of negative allosteric modulators. *Mol Pharmacol* **70**:616–626.
- Hong YH, Nishimura Y, Hishikawa D, Tsuzuki H, Miyahara H, Gotoh C, Choi KC, Feng DD, Chen C, Lee HG, et al. (2005) Acetate and propionate short chain fatty acids stimulate adipogenesis via GPCR43. *Endocrinology* **146**:5092–5099.
- Jacobson MP, Pincus DL, Rapp CS, Day TJ, Honig B, Shaw DE, and Friesner RA (2004) A hierarchical approach to all-atom protein loop prediction. *Proteins* **55**:351–367.
- Kaminski GA, Friesner RA, Tirado-Rives J, and Jorgensen WL (2001) Evaluation and reparameterization of the OPLS-AA force field for proteins via comparison with accurate quantum chemical calculations on peptides. *J Phys Chem B* **105**:6474–6487.
- Kollias-Baker CA, Ruble J, Jacobson M, Harrison JK, Ozeck M, Shryock JC, and Belardinelli L (1997) Agonist-independent effect of an allosteric enhancer of the A1 adenosine receptor in CHO cells stably expressing the recombinant human A1 receptor. *J Pharmacol Exp Ther* **281**:761–768.
- Langmead CJ and Christopoulos A (2006) Allosteric agonists of 7TM receptors: expanding the pharmacological toolbox. *Trends Pharmacol Sci* **27**:475–481.
- Le Poul E, Loison C, Struyf S, Springael JY, Lannoy V, Decobecq ME, Brezillon S, Dupriez V, Vassart G, Van Damme J, et al. (2003) Functional characterization of human receptors for short chain fatty acids and their role in polymorphonuclear cell activation. *J Biol Chem* **278**:25481–25489.
- Leppik RA and Birdsall NJ (2000) Agonist binding and function at the human α_{2A} -adrenoceptor: allosteric modulation by amilorides. *Mol Pharmacol* **58**:1091–1099.
- Lundquist F, Tygstrup N, Winkler K, Mellemgaard K, and Munck-Petersen S (1962) Ethanol metabolism and production of free acetate in the human liver. *J Clin Invest* **41**:955–961.
- Lundstrom K (2006) Latest development in drug discovery on G protein-coupled receptors. *Curr Protein Pept Sci* **7**:465–470.
- May LT, Leach K, Sexton PM, and Christopoulos A (2007) Allosteric modulation of G protein-coupled receptors. *Annu Rev Pharmacol Toxicol* **47**:1–51.
- Nemeth EF, Heaton WH, Miller M, Fox J, Balandrin MF, Van Wagenen BC, Colloton M, Karbon W, Scherrer J, Shatzin E, et al. (2004) Pharmacodynamics of the type II calcimimetic compound cinacalcet HCl. *J Pharmacol Exp Ther* **308**:627–635.
- Nilsson NE, Kotarsky K, Owman C, and Olde B (2003) Identification of a free fatty acid receptor, FFA2R, expressed on leukocytes and activated by short-chain fatty acids. *Biochem Biophys Res Commun* **303**:1047–1052.
- Ponder JW and Richards FM (1987) An efficient Newton-like method for molecular mechanics energy minimization of large molecules. *J Comput Chem* **8**:1016–1024.
- Prilla S, Schrobang J, Ellis J, Hölte HD, and Mohr K (2006) Allosteric interactions with muscarinic acetylcholine receptors: complex role of the conserved tryptophan M2422Trp in a critical cluster of amino acids for baseline affinity, subtype selectivity, and cooperativity. *Mol Pharmacol* **70**:181–193.
- Rayasam GV, Tulasi VK, Davis JA, and Bansal VS (2007) Fatty acid receptors as new therapeutic targets for diabetes. *Exp Opin Ther Targets* **11**:661–671.
- Sawzdargo M, George SR, Nguyen T, Xu S, Kolakowski LF, and O'Dowd BF (1997) A cluster of four novel human G protein-coupled receptor genes occurring in close proximity to CD22 gene on chromosome 19q13.1. *Biochem Biophys Res Commun* **239**:543–547.
- Siler SQ, Neese RA, and Hellerstein MK (1999) De novo lipogenesis, lipid kinetics, and whole-body lipid balances in humans after acute alcohol consumption. *Am J Clin Nutr* **70**:928–936.
- Soga T, Kamohara M, Takasaki J, Matsumoto S, Saito T, Ohishi T, Hiyama H, Matsuo A, Matsushime H, and Furuichi K (2003) Molecular identification of nicotinic acid receptor. *Biochem Biophys Res Commun* **303**:364–369.
- Still WC, Tempczyk A, Hawley RC, and Hendrickson T (1990) Semianalytical treatment of solvation for molecular mechanics and dynamics. *J Am Chem Soc* **112**:6127–6129.
- Sum CS, Tikhonova IG, Neumann S, Engel S, Raaka BM, Costanzi S, and Gershengorn MC (2007) Identification of residues important for agonist recognition and activation in GPR40. *J Biol Chem* **282**:29248–29255.
- Tränkle C, Dittmann A, Schulz U, Weyand O, Buller S, Jöhren K, Heller E, Birdsall NJ, Holzgrabe U, Ellis J, et al. (2005) Atypical muscarinic allosteric modulation: cooperativity between modulators and their atypical binding topology in muscarinic M2 and M2/M5 chimeric receptors. *Mol Pharmacol* **68**:1597–1610.
- Tränkle C, Weyand O, Voigtländer U, Mynett A, Lazareno S, Birdsall NJ, and Mohr K (2003) Interactions of orthosteric and allosteric ligands with [³H]dimethyl-W84 at the common allosteric site of muscarinic M2 receptors. *Mol Pharmacol* **64**:180–190.
- Tunaru S, Kero J, Schaub A, Wufka C, Blaukat A, Pfeffer K, and Offermanns S (2003) PUMA-G and HM74 are receptors for nicotinic acid and mediate its antilipolytic effect. *Nat Med* **9**:352–355.
- Urwiler S, Mosbacher J, Lingenhoehl K, Heid J, Hofstetter K, Froestl W, Bettler B, and Kaupmann K (2001) Positive allosteric modulation of native and recombinant gamma-aminobutyric acid(B) receptors by 2,6-di-tert-butyl-4-(3-hydroxy-2,2-dimethyl-propyl)-phenol (CGP7930) and its aldehyde analog CGP13501. *Mol Pharmacol* **60**:963–971.
- Wise A, Foord SM, Fraser NJ, Barnes AA, Elshourbagy N, Eilert M, Ignar DM, Murdock PR, Steplewski K, Green A, et al. (2003) Molecular identification of high and low affinity receptors for nicotinic acid. *J Biol Chem* **278**:9869–9874.

Address correspondence to: Yang Li, Amgen Inc., 1120 Veterans Blvd, South San Francisco, CA 94080. E-mail: yangli@amgen.com